

CODEPLOT-COT: MATHEMATICAL VISUAL REASONING BY THINKING WITH CODE-DRIVEN IMAGES

Chengqi Duan^{1*} **Kaiyue Sun^{1*}** **Rongyao Fang^{3*}** **Manyuan Zhang^{2†}** **Yan Feng²** **Ying Luo²**
Yufang Liu² **Ke Wang³** **Peng Pei²** **Xunliang Cai²** **Hongsheng Li³** **Yi Ma¹** **Xihui Liu^{1‡}**

¹HKU ²Meituan ³CUHK

(1) Comparison of Mathematical Reasoning Benchmarks

Text-centric (MATH-500)

Find the greatest integer less than $(\sqrt{7} + \sqrt{5})^6$

Answer (in pure text):
13535

- Multimodal (MathVista)

Question (multimodal):
 \overline{AB} is a diameter, $AC = 8$ inches, and $BC = 15$ inches.
Find the radius of the circle.

Answer (in pure text)
8.5

----- Visual Reasoning (Our Math-VR) -----

Question (in pure text or multimodal):
In an isosceles triangle with legs of length 5 and with a height of 4 from one vertex, find the length of the base.
Multimodal Reasoning:

Answer: 6 $2\sqrt{5}$ $4\sqrt{5}$

Answer: 6 $2\sqrt{5}$ $4\sqrt{5}$

(2) Method Comparison: Reasoning Processes on a Visual Reasoning Problem

Math-VR

Question:
Find the area of the quadrilateral ABCD, given $AB=4$, $BC=3$, $DC=12$, $AD=13$, and $\angle B=90^\circ$.

-- LLM/VLM (Text Reasoning) --



Response:
 The total area of the quadrilateral is the sum of the areas of the two triangles.
 $\text{Area}(\text{ABCD}) = \text{Area}(\triangle \text{ABC}) + \text{Area}(\triangle \text{ADC})$
 $\text{Area}(\text{ABCD}) = 6 + 30$
 $\text{Area}(\text{ABCD}) = 36$

The area of the quadrilateral ABCD is **36** square units.

Unified Model (Text & Image)



- CodePlot-CoT (Our Method)

```
Response:  
I will generate code to plot the  
geometry.  
↓(Generated by VLM)
```

The diagram shows a triangle ABC with vertices A , B , and C . A dashed vertical line segment extends from vertex B down to the base AC , meeting it at point D . This line segment creates two new triangles: $\triangle ABD$ and $\triangle CBD$. The angle at vertex B in triangle ABC is labeled $\angle B$. The angle at vertex B in triangle CBD is also labeled $\angle B$. The angle at vertex D in triangle ABD is labeled $\angle ADB$.

Figure 1: A comparison of mathematical reasoning benchmarks and the methods on the visual reasoning problem. (1) illustrates that unlike existing benchmarks that rely on textual reasoning, Math-VR requires deep visual reasoning to resolve the math problems. (2) shows that on a visually ambiguous problem from Math-VR, both text-only and unified multimodal models fail. Our method, CodePlot-CoT, succeeds by programmatically generating the figure to uncover its true geometric properties, thus arriving at the correct solution.

ABSTRACT

Recent advances in Large Language Models (LLMs) and Vision Language Models (VLMs) have shown significant progress in mathematical reasoning, yet they still face a critical bottleneck with problems requiring visual assistance, such as drawing auxiliary lines or plotting functions to solve the problems. Most LLMs and VLMs are constrained to text-only reasoning chains, while multimodal unified models that can generate interleaved text and images lack the necessary precision and controllability for such tasks. To address this, we propose **CodePlot-CoT**, a code-driven Chain-of-Thought paradigm for “thinking with images” in mathematics. Our approach leverages the VLM to generate text reasoning as well as executable plotting code, which is then rendered into images as “visual thought”, to solve mathematical problems. To achieve this, we first construct **Math-VR**, the first large-scale, bilingual dataset and benchmark for Mathematics problems with Visual Reasoning, comprising 178K samples. Second, to create high-quality training data, we develop a state-of-the-art image-to-code converter specialized for parsing complex mathematical figures into codes. Finally, using these training data, we train the CodePlot-CoT model for solving mathematical problems. Experimental results show that our model achieves up to **21%**

*Equal Contribution

[†]Project Lead

[†]Corresponding Author

increase over base model on our new benchmark, fully validating the efficacy of our proposed code-driven reasoning paradigm. Our work opens a new direction for multimodal mathematical reasoning and provides the community with the first large-scale dataset, comprehensive benchmark, and strong approach for such problems. To facilitate future research, we make our datasets, code, and pre-trained models publicly available at <https://github.com/HKU-MMLab/Math-VR-CodePlot-CoT>.

“Algebra is but written geometry and geometry is but figured algebra.”
– Sophie Germain

1 INTRODUCTION

Human cognition is inherently multimodal, leveraging visual graphs, diagrams, and sketches to facilitate complex reasoning. This is particularly evident in mathematics, where such visual aids—from drawing auxiliary lines in geometric proofs to plotting functions—are essential for rendering abstract relationships concrete and making the reasoning process more intuitive (Hu et al., 2024). While recent advances in Vision Language Models (VLMs) have shown strong performance in mathematical reasoning (Gao et al., 2023a; Shi et al., 2024; Zhang et al., 2024b), they typically rely on text-only reasoning chains. This becomes a major limitation for problems that require visual reasoning, where humans would simply sketch diagrams or add auxiliary lines to facilitate reasoning. Such deficiency in multimodal reasoning leads to redundant and even incorrect text-only reasoning in mathematical problem solving (shown in Figure 1).

Recent efforts in general-domain visual understanding have explored the paradigm of Visual Chain-of-Thought (Visual CoT) (Shao et al., 2024), attempting to realize it by directly generating and manipulating images (Li et al., 2025b; Chen et al., 2025; Li et al., 2025a). However, this paradigm breaks down in the context of mathematics problems that demand high precision, where naive image generation is insufficient. Even state-of-the-art unified models struggle to execute precise operations in mathematics, such as constructing auxiliary lines that satisfy strict geometric constraints.

The fundamental challenge in direct image generation and manipulation arises from the inherent difficulty in modeling the high-dimensional distribution of natural images, which contain complex textures and high-frequency details. However, mathematical visual aids differ significantly from general image generation tasks: the critical aspect is not the pixel-level details or textures, but rather the precise representation of key structured geometric properties such as shapes, lengths, positions, and angular relationships. This distinction suggests that the essential information in mathematical figures can be better captured by structured representations rather than pixel-level encodings. Therefore, we introduce programmatic code as the optimal representation for mathematical visual reasoning. As an inherently textual and structured representation format, code aligns seamlessly with language models (Surís et al., 2023; Wang et al., 2025a; 2023), enabling straightforward generation without introducing complex distributional modeling (e.g., diffusion models).

In this work, we propose a new paradigm that enables VLMs to engage in visual reasoning through code generation. Instead of directly generating images with VLMs, which typically leads to degraded quality and precision in math plots, our approach guides the model to output executable plotting codes which are rendered into images as intermediate “visual thoughts”. Once executed, the generated code produces images that can be input back into the VLM reasoning sequence.

Implementing this paradigm requires addressing two key challenges. First, there is a lack of structured dataset and benchmark for mathematical problems that demand visual reasoning, as existing works focus mainly on interpreting given figures rather than reasoning with visual images during problem solving (Lu et al., 2023; Zhang et al., 2024a). Therefore, we construct Math-VR, a large-scale bilingual dataset and benchmark comprising 173K training, 5K testing mathematical problems with visual reasoning solutions. We then benchmark existing SOTA models, thereby establishing strong baselines and highlighting the difficulty of this new task. Second, training models to output code as representations of visual thought requires a bidirectional mapping between code and images. We tackle this by developing MatplotCode, a high-fidelity image-to-code converter, which we leverage to construct code-driven CoT for training. The curated data then serves as the foundation

for training CodePlot-CoT, a model specialized for code-driven visual reasoning. Our experiments show that it achieves up to 21% increase over base model, validating the efficacy of our approach.

The main contributions of our work can be summarized as follows:

- We propose a novel and efficient paradigm that enables VLMs to engage in visual reasoning through code generation.
- We construct **Math-VR**, the first large-scale, bilingual dataset and benchmark (178K samples) for Mathematical problems with Visual Reasoning.
- We develop **MatplotCode**, a state-of-the-art image-to-code converter for mathematical figures, and train **CodePlot-CoT** model, a specialized model that achieves up to a 21% performance increase over strong baselines.

2 RELATED WORK

VLMs in Mathematics Reasoning. Reasoning greatly enhances model performance in general tasks. (Wei et al., 2022; Fang et al., 2025; Duan et al., 2025) Recent progress on multimodal mathematical reasoning largely follows two lines: scaling math-specific multimodal data and improving architectures for visual–text alignment. Representative data-centric efforts include G-LLaVA (Gao et al., 2023a) with a geometry-focused corpus (Geo170K), Math-LLaVA (Shi et al., 2024) with the large-scale MathV360K, and MAVIS (Zhang et al., 2024b) which further optimizes math-specific visual encoding and provides auto-generated CoT rationales. To evaluate these developments, benchmarks such as MathVista (Lu et al., 2023), MathVerse (Zhang et al., 2024a), Math-Vision (Wang et al., 2024), and MV-Math (Wang et al., 2025b) have emerged, each targeting different aspects of mathematical reasoning in visual contexts. Despite these advances, existing studies have mainly focused on understanding given visual inputs, rather than incorporating visual information into the reasoning chain (plotting auxiliary lines or functions in solutions etc.).

“Thinking with image” Models. To overcome the limitations of text-only reasoning, recent research focuses on “Thinking with image,” or Visual Chain-of-Thought (VCoT), where models actively retrieve or generate visual aids in reasoning process. Several works (Corbière et al., 2025; Jiang et al., 2025; Zhang et al., 2025; OpenAI, 2025b; Surís et al., 2023; Shao et al., 2024) implement a multimodal chain of thought where they retrieve and crop from the input image and interleave these visual snippets into the reasoning chain to provide more focused context for subsequent VQA steps. Other works (Li et al., 2025a;b; Chern et al., 2025; Pan et al., 2025) focus on building unified models capable of generating interleaved text and image reasoning chain auto-regressively. These approaches discretize or embed images into visual tokens and train a single sequence model that sequentially outputs text and image during decoding. The generated images can serve as visual feedback for navigation tasks like mazes.

Visual Reasoning Models in Mathematics. Contemporary visual reasoning models for mathematics predominantly follow two paradigms: interleaved “thinking with image” (Li et al., 2025a; Chen et al., 2025; Wang et al., 2025d) and agent-plus-code tool use (Hu et al., 2024; Gao et al., 2023b; Zhou et al., 2023). Interleaved approaches enable the model to sequentially add auxiliary lines and plot functions. However, the visual actions are weakly controllable, which hampers precise geometric constructions and limits the interpretability of intermediate reasoning steps. The agent-plus-code paradigm treats the model as a planner that create and manipulate input figure by predicting code snippets and call to external tools (Python, CAS/solver libraries, plotting utilities etc.). The executed outputs are again inputted to the model as visual feedback. In contrast to interleaved generation, tool-augmented agents provide precise and verifiable outputs by executing code, yet their performance largely depends on the reliability of the planner. Current planners are often zero-shot and not specifically trained for mathematical reasoning, which makes them susceptible to producing fragile or incorrect tool-use sequences.

3 MATH-VR: DATASET AND BENCHMARK FOR MATH VISUAL REASONING

3.1 MATHEMATICAL PROBLEMS REQUIRE VISUAL REASONING

Previous mathematical benchmarks, such as Math-500 (vals.ai, 2025b), AIME (vals.ai, 2025a), and HMMT (MathArena, 2025), primarily evaluate models’ textual reasoning abilities. More recent efforts like MathVista (Lu et al., 2023) and MATH-Vision (Wang et al., 2024) introduce a multimodal setting by incorporating image-based questions. However, their focus remains largely on visual perception and extracting information from images, and the reasoning processes are still text-only reasoning without introducing visual thoughts.

We argue that visual reasoning in mathematics should be an active process of “reasoning with images”, which motivates us to propose a new benchmark, Math-VR. Figure 1(a) illustrates the distinction between existing benchmarks and ours. Previous benchmarks’ reasoning can be performed entirely in text, whereas Math-VR necessitates multimodal reasoning with images. For example, the isosceles triangle problem shown in Figure 1(a) requires considering three possible scenarios. Moving beyond naive visual perception, Math-VR demands solvers to conduct reasoning in both text and image domains, such as adding auxiliary lines, to assist with solving math problems.

3.2 DATASET CONSTRUCTION

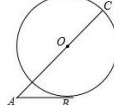
Dataset Collection and Filtering. We begin with collecting 900k secondary-school-level math problems with solutions from public websites, each containing at least one image in explanation (reasoning process) of the solution. Using Qwen2.5-VL-72B, we filter out irrelevant or purely textual images and retain only samples that require mathematical figures for reasoning. Furthermore, we employ GPT-4.1 to convert textual images into readable text and standardize each question into Markdown format. GPT-4.1 further conducts quality checks to discard incomplete or incoherent questions. This process results in **Math-VR dataset**, the first large-scale dataset targeted for visual mathematical reasoning, comprising 178,150 bilingual (English and Chinese) samples.

Dataset Statistics. In Math-VR dataset, each sample consists of a question, a reasoning process, and a final answer, with at least one image in the reasoning process. Math-VR encompasses a wide variety of visual reasoning tasks, with 29% text-only and 71% multimodal questions, spanning domains such as Geometry, Algebra, Calculus, and Statistics, where Geometry dominates (81%), and is hierarchically categorized into subdomains and knowledge points (*e.g.*, Triangle, Circle, Quadrilateral, Area, and Perimeter). More details about our dataset collection, categorization, and statistics are presented in Appendix.

Visualization of Math-VR dataset. Figure 2 presents a visualization of Math-VR sample. Each sample in Math-VR contains both textual and visual reasoning. The visual figures in the analysis depict key geometric relations or intermediate steps, helping to clarify the reasoning process and demonstrate how image-based reasoning complements textual explanation. Additional examples are shown in Figure 10 and 11 in Appendix.

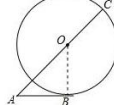
Question:

As shown, AB is a tangent to $\odot O$ at point B , and the extension of AO meets $\odot O$ at point C . If $\angle A = 45^\circ$ and $AB = 2$, then AC equals ()?



Analysis:

Connect OB , then $\triangle AOB$ is a right triangle. Using trigonometry, we can find the length of OA , so AC can be determined.



Since AB is a tangent to $\odot O$ at point B , Thus $OB \perp AB$.

In right triangle OAB : $OB = AB \cdot \tan A = 2 \times \tan 45^\circ = 2$; So $OA = \sqrt{OB^2 + AB^2} = \sqrt{2^2 + 2^2} = \sqrt{8} = 2\sqrt{2}$, So $AC = OA + OC = OA + OB = 2\sqrt{2} + 2$.

Therefore, the answer is $2\sqrt{2} + 2$.

Figure 2: Visualization of Math-VR sample.

Table 1: **Key Statistics for Math-VR Benchmark.** We report statistics of our benchmark, including token lengths of questions and solutions, as well as the number and resolution of images.

Statistics	Number
Question Length (text tokens)	
- Minimum	9
- Maximum	602
- Average	144.23
Solution Length (text tokens)	
- Minimum	46
- Maximum	2753
- Average	591.14
# Images in Each Question	
- Maximum number	4
- Average number	1.04
- Average resolution	320x320
# Images in Each Solution	
- Maximum number	7
- Average number	1.24
- Average resolution	305x305

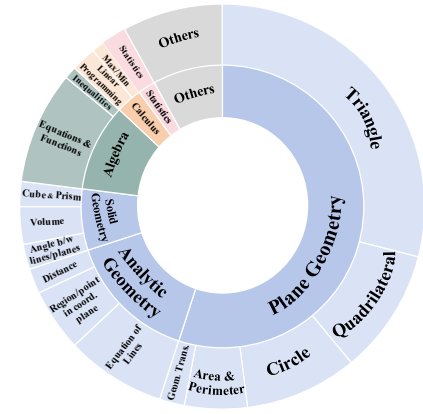


Figure 3: **Distribution of Knowledge Types in Math-VR Benchmark.** Geometry constitutes the majority of problems (77%), with Algebra and Calculus comprising 13%.

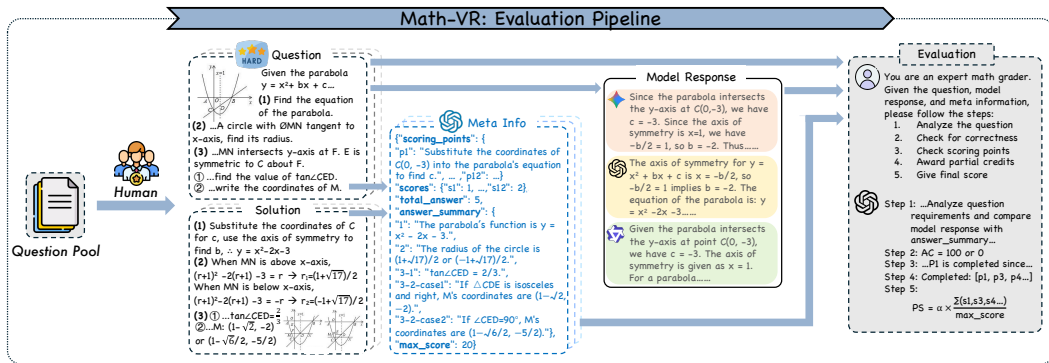


Figure 4: **Math-VR Evaluation Pipeline.** We design a VLM-based framework to comprehensively assess visual reasoning abilities of different models. The evaluation uses two metrics: Answer Correctness (AC), which gives a reliable binary judgment of the final answer, and Process Score (PS), which provides a fine-grained assessment of the solving process.

3.3 BENCHMARK AND EVALUATION

Benchmark Construction. To evaluate the visual mathematical reasoning capabilities of different models, we develop the Math-VR benchmark, which consists of 5k bilingual mathematical questions drawn from our dataset. The questions in Math-VR are selected through a careful pipeline designed to ensure a deterministic and reliable evaluation. First, proof-based questions are excluded to avoid the difficulty and bias of assessing the logical validity. Most multiple-choice questions are excluded, since random guessing can yield correct answers by chance. From the remaining questions, a random pool of 3,000 samples was drawn from our dataset and manually reviewed to remove questions that require minimal or trivial visual reasoning.

Benchmark Statistics and Distribution. Our Math-VR benchmark is divided into two subsets: the Text subset, containing 2k text-only questions, and the Multimodal subset, comprising 3k questions that are demonstrated with both text and mathematical images. Both subsets require reasoning or imagination in the visual domain to solve the questions. Table 1 and Figure 3 summarize the statistics and distribution of knowledge types of Math-VR benchmark, respectively.

Evaluation Metrics. Figure 4 illustrates the evaluation pipeline of Math-VR, where GPT-4.1 (OpenAI, 2025a) is employed as the VLM evaluation tool. We design two metrics: Answer Correctness (AC) and Process Score (PS). Given the free-form nature of the answers (e.g., multiple numbers,

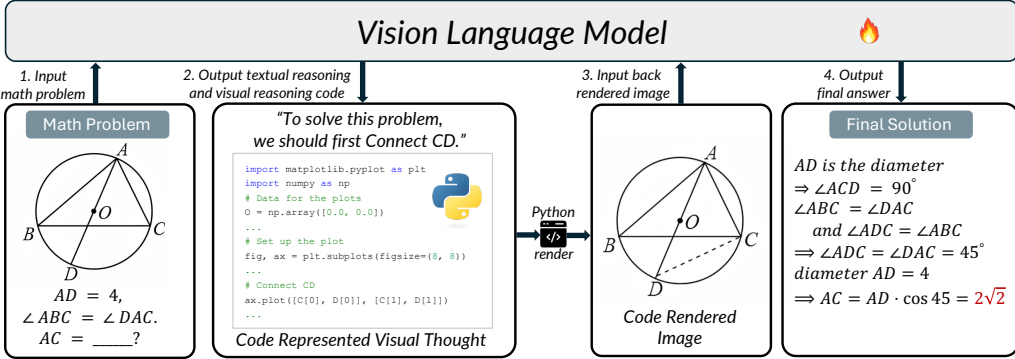


Figure 5: **Illustration of the CodePlot-CoT paradigm for mathematical visual reasoning.** The model interleaves natural language reasoning with code-based visual reasoning. At points in the solution that require visual support, the model generates a sequence of executable plotting code, which is rendered via Python into precise figures and input back into the model. This allows the model to “see” its own visual thought and leverage it for subsequent reasoning, ultimately leading to a more accurate final solution. CodePlot-CoT supports interleave text and multi-image reasoning.

ranges, or short text responses), we first use the VLM to analyze the ground-truth solution and generate a comprehensive summary of the final answer for each question. Simultaneously, the VLM is prompted to identify “scoring points” within the solution. These scoring points refer to the critical steps required to solve the problem, such as applying theorems, making necessary deductions, and performing calculations. Each scoring point is assigned a value reflecting its difficulty (e.g., 1 or 2). These extracted answers and scoring points serve as a reference to compare with the model-generated responses during evaluation.

(1) Answer Correctness (AC): To ensure consistent, reproducible, and objective evaluation results, this metric strictly checks whether the model-generated answer matches the ground-truth answer. If the answer is completely correct, it receives a score of 1 for AC; any error or omission results in a score of 0.

(2) Process Score (PS): When solving mathematical questions, even if the final answer is incorrect, the reasoning process may still be meaningful. This metric awards partial credit if the model hits several scoring points in the reasoning process but fails to achieve the completely correct final answer. If a final answer is completely correct (*i.e.*, AC=100), then it automatically receives a PS of 100. Otherwise, PS for a question q is defined as follows:

$$PS(q) = \alpha \times \frac{\sum_{j=1}^m v_j}{\sum_{i=1}^n v_i} \times 100, \text{ when the answer is not fully correct} \quad (1)$$

where α represents a discount factor, we take $\alpha = 0.7$. n is the total number of scoring points for the question. m is the number of scoring points hit by the model answer. v_j is the point value of the j -th scoring point.

We have conducted a manual review of the VLM summarized information for each sample in our benchmark. For more details about the manual verification and the templates used for prompting GPT-4.1, please refer to the Appendix.

4 CODEPLOT-COT PARADIGM: CODE-DRIVEN CoT FOR MATHEMATICS VISUAL REASONING

4.1 PARADIGM OVERVIEW

Existing VLMs remain constrained when visual aids are required. Most models still rely primarily on text-only chain-of-thought reasoning, which often fails to capture complex visual elements and

geometric properties. To address this, recent efforts introduce Visual CoT by directly generating or manipulating images. However, it is difficult for current image generation models to satisfy strict geometric constraints in the mathematical context. These shortcomings constitute fundamental obstacles to accurate visual reasoning in mathematics.

To overcome these limitations, we propose CodePlot-CoT, which represents “visual thoughts” as executable plotting code instead of pixel-encoded images. Our key insight is to replace pixel-level visual generation and manipulation with a language modeling problem: instead of “drawing” in visual space, the VLM can “write” code in the text modality where it is inherently proficient. Mathematical figures do not rely on pixel-level fidelity or texture details. Instead, what matters are the structural attributes such as geometric shapes, spatial positions, and angular relations, making executable plotting code a perfect fit for representing such structured geometric information. By releasing the burden of pixel-level distribution modeling, the model can concentrate on the precise geometric information, making it easier to reason with mathematical figures.

Figure 5 presents the CodePlot-CoT paradigm, where text reasoning is interleaved with code-based visual reasoning. The model first generates a reasoning chain in natural language. When visual reasoning step is necessary (such as constructing an auxiliary line), it generates a block of plotting code that represents the required visual information. This code is executed to render an image, which is then input back to the model as the visual reasoning. Such visual thought allows the model to ground its subsequent reasoning in precise, self-generated visual evidence. This fundamentally changes the nature of the model’s reasoning, moving it beyond text-only reasoning to a multimodal reasoning chain where thoughts and hypotheses are proposed, tested, and refined in both visual and linguistic domains.

4.2 CODE-DRIVEN COT CURATION WITH IMAGE-TO-CODE CONVERTER

A core prerequisite for training CodePlot-CoT is the high-quality data that integrates images, plotting code, and reasoning chains as presented in Figure 5. Such data allows the model to learn how visual thoughts can be faithfully represented as executable code. However, existing mathematical resources rarely provide paired code annotations for visual reasoning, making it difficult to obtain the structured supervision required for code-driven CoT. This motivates the need for a reliable image-to-code mapping that can convert mathematical figures to plotting code. Yet, no fine-grained converter specialized for this domain is publicly available. Even large commercial models (e.g., Gemini-2.5-Pro, GPT-5) are unreliable for zero-shot image-to-code conversion on complex mathematical figures, limiting practical effectiveness. To overcome this bottleneck, we develop **MatplotCode**, a state-of-the-art converter tailored for mathematical figures, which enables scalable creation of code–image pairs and supports the curation of supervised fine-tuning data for CodePlot-CoT.

We leverage the ImgCode-8.6M dataset from MathCoder-VL (Wang et al., 2025a) as the foundation of our experiment. We begin by filtering out images that are not representative of standard mathematical figures, thereby curating a high-quality subset focused on geometry diagrams and function plots. All code representations in this dataset are in Python. On this curated data, we train MatplotCode, which demonstrates superior generalization and conversion fidelity. To further enhance the quality of our supervised fine-tuning data, we use MatplotCode to generate multiple Python code representations for each source image and employ GPT-4.1 to select the optimal representation.

4.3 TRAINING DETAILS

We leverage Qwen2.5VL-32B as the base model for both MatPlotCode and CodePlot-CoT model. MatPlotCode goes through a two-stage training process: we first align the visual components by training only the vision encoder (ViT) and the MLP projector for one epoch, and then perform full-parameter fine-tuning for two additional epochs. For the CodePlot-CoT model, we initialize its weights from vision-aligned MatPlotCode after Stage 1. We then fully finetune this model on our curated SFT dataset for 5000 steps. During MatPlotCode training, we assign loss to the textual reasoning chain and generated code while no loss is applied to the rendered images in the sequence. More details on our training are presented in the Appendix.

5 EXPERIMENTS

5.1 HUMAN CORRELATION ANALYSIS

To further validate the reliability of our automatic evaluation pipeline, we conduct a human correlation study. We invite 15 senior undergraduate students majoring in STEM disciplines as our human experts. We then randomly sample 1000 questions from our benchmark and generate a total of 3000 answers from GPT4.1, Gemini-2.5-pro and Claude-Sonnet-4. Each participant is assigned 200 answers and is asked to (i) judge the Answer Correctness (AC) in a correct/incorrect manner and (ii) assign a Process Score (PS) based on the same scoring point in our benchmark. Both scores show strong consistency between human annotations and GPT-4.1 evaluations.

- **Answer Correctness (AC):** We report Cohen’s $\kappa = 0.75$ and MCC = 0.75. For binary judgments, beyond simple accuracy, these measures account for chance agreement and balance between positive/negative classes.
- **Process Score (PS):** We report Pearson $r = 0.72$ and Spearman $\rho = 0.70$. Pearson captures the linear correlation between human and GPT-4.1 scores, while Spearman focuses on rank-order consistency.

5.2 BENCHMARKING EXISTING MODELS AND CODEPLOT-COT ON MATH-VR

For a comprehensive evaluation, we compare our approach against a suite of state-of-the-art LLMs, VLMs, or UMs, including both open-source and closed-source ones on the 2500 English questions in our benchmark, as shown in Table 2. Among closed-source and large open-source models, Gemini-2.5-Pro stands out, achieving the highest overall scores (PS = 80.8, AC = 64.7) on the Math-VR. We observe that “thinking” models which benefit from better-structured textual chains performs better on our benchmark. Among no-thinking models, Nano Banana achieves the highest score, primarily due to its stronger visual reasoning capabilities rather than purely text-based chains. Nevertheless, there remains substantial space for improvement in Answer Correctness across closed-source models. Even the strongest performer, Gemini-2.5-Pro, still fails on approximately one-third of the benchmark problems. This gap highlights that current advances in chain length and scale alone are insufficient, and points toward future research directions in developing more faithful and controllable visual reasoning mechanisms.

The limitations are more significant in open-source models under 100B, most of which remain constrained to pure text reasoning and consequently exhibit low answer correctness on Math-VR benchmark (e.g., Gemma, Qwen2.5-VL-72B). Attempts to “think with images” by directly generating pixels (e.g., Bagel-Zebra-CoT) provide only modest gains due to poor controllability and low geometric precision due to model scale. In contrast, our code-driven approach yields substantial improvements: CodePlot-CoT surpasses its 32B base VLM by up to 21% and largely outperforms the Qwen2.5-VL-72B across all metrics, demonstrating that structured, verifiable visual reasoning is more decisive than model size or longer textual chains. CodePlot-CoT generated examples are shown in Figure 12 and 13 in Appendix.

5.3 IMAGE-CODE CONVERTER EVALUATION

We evaluate MatplotCode against FigCodifier-8B, GPT-o3 and Gemini-2.5-pro (thinking budget maximum). We randomly sample 1000 images from our dataset and task these models to convert it to matplotlib code. We assess two aspects: (i) Execution Success Rate, i.e., the probability that the generated code runs without errors. (ii) Reconstruction Fidelity, judged by GPT-4.1 via a standardized prompt to decide which reconstruction is most similar to the original image. The full evaluation prompt is provided in the Appendix.

Both MatplotCode and the FigCodifier-8B achieve a 100% execution success rate. In contrast, GPT-o3 reach 79.6%, while Gemini-2.5-Pro achieve 86.2%, indicating a higher likelihood of producing invalid or incomplete code. For reconstruction fidelity, judged by GPT-4.1, MatplotCode is preferred in 554 out of 1,000 cases, compared to 190 for FigCodifier-8B, 49 for GPT-o3, and 207 for Gemini-2.5-Pro. These results demonstrate that our converter not only guarantees reliable code prediction, but also produces reconstructions that are consistently closer to the original figures. Importantly, the

Table 2: **Math-VR evaluation results.** This table compares the model performances on our benchmark. The second column specifies the model size by its parameter count. For models that support an internal reasoning process, \checkmark in the “Thinking” column indicate this mode is turned on during evaluation. Model Types: VLM: Vision Language Model, LLM: Large Language Model, UM: Unified Model. Metrics: PS: Process Score, AC: Answer Correctness. Blue and Yellow highlight the top score in each model group. **Bold** signifies the highest score across all models.

Model	# Params	Type	Think	Text		Multimodal		Overall	
				PS	AC	PS	AC	PS	AC
<i>Closed-source Models and Open-source Models over 100B</i>									
GPT-4o(2024)	-	VLM	\times	34.6	5.7	27.6	3.4	30.4	4.3
GPT-4.1-nano(2025a)	-	VLM	\times	45.9	13.1	33.6	6.4	38.5	9.1
GPT-4.1-mini(2025a)	-	VLM	\times	62.0	33.3	58.6	33.3	60.0	33.3
GPT-4.1(2025a)	-	VLM	\times	56.5	26.6	52.2	25.6	53.9	26.0
GPT-o3(2025b)	-	VLM	\checkmark	72.9	52.9	78.6	63.7	76.4	59.3
Gemini-2.0-Flash(2024)	-	VLM	\times	56.1	24.1	47.0	18.3	50.7	20.6
Gemini-2.5-Flash(2025)	-	VLM	\times	70.9	44.6	75.5	57.5	73.7	52.3
Gemini-2.5-Flash(2025)	-	VLM	\checkmark	77.5	57.0	79.0	62.9	78.4	60.5
Gemini-2.5-Pro(2025)	-	VLM	\checkmark	77.9	58.7	82.8	68.7	80.8	64.7
Nano Banana(2025)	-	UM	\times	72.3	49.1	74.7	56.3	73.8	53.4
Seed-1.6-Thinking(2025)	-	VLM	\checkmark	73.0	53.0	76.6	62.0	75.2	58.4
Claude-Sonnet-4(2025)	-	VLM	\times	60.9	31.5	53.4	25.8	56.4	28.1
GLM-4.5V(2025)	108B	VLM	\checkmark	70.5	48.0	69.1	50.6	69.7	49.6
Deepseek-R12025	671B	LLM	\checkmark	69.9	49.5	-	-	-	-
<i>Open-source Models under 100B</i>									
Bagel(2025)	7B	UM	\times	32.9	8.5	24.0	7.0	27.6	7.6
Bagel-Zebra-CoT(2025a)	7B	UM	\times	41.5	13.9	29.1	7.6	34.1	10.1
Keye-VL-1.5(2025)	8B	VLM	\times	44.4	20.2	34.0	15.4	38.2	17.3
InternVL-3.5-8B(2025c)	8B	VLM	\times	35.6	9.2	28.6	7.0	31.4	7.9
Gemma3(2025)	27B	VLM	\times	50.8	19.2	40.8	14.1	44.8	16.1
Qwen-2.5-VL-3B(2025)	3B	VLM	\times	33.4	7.9	23.6	3.6	27.5	5.3
Qwen-2.5-VL-7B(2025)	7B	VLM	\times	18.0	4.5	11.0	2.0	13.8	3.0
Qwen-2.5-VL-32B(2025)	32B	VLM	\times	36.9	10.6	31.5	9.6	33.7	10.0
Qwen-2.5-VL-72B(2025)	72B	VLM	\times	44.6	15.3	38.2	12.7	40.8	13.7
CodePlot-CoT	32B	VLM	\times	53.8	31.6	42.4	15.8	47.0	22.1
Δ Over Base Model				+16.9	+21.0	+10.9	+6.2	+13.3	+12.1

failures of both closed-source large models and open-source expert models further underscore the necessity of developing a new converter tailored to this task.

5.4 ANALYSIS ON INFERENCE COST

In this section, we analyze the inference cost of our code-driven visual reasoning paradigm. On the 2,500 test problems, our model generates an average of 820.9 tokens per image and 3,416 rendered images in total, or 1.37 images per problem on average. From the perspective of token usage, this cost is lower than many autoregressive “thinking with image” models, which typically consume 1,024 or even up to 4,096 tokens per image. Moreover, each image can be rendered locally in less than one second, making it negligible when evaluating overall computational efficiency. We further measure the total number of output tokens. On average, our model produces 567.2 text tokens, and together with the code tokens for rendered images, the overall output is 1,691.8 tokens per problem. In comparison, Qwen2.5-VL-32B generates substantially more content, averaging 3,847.3 tokens. This significant reduction in output length highlights the efficiency of our code-driven visual reasoning paradigm on Math-VR.

Table 3: Comparing our code-driven paradigm against text-only reasoning. Qwen-2.5VL-3B-Text-Tune is fine-tuned on text-only CoT, while CodePlot-CoT-3B is trained with our paradigm. The results demonstrate the significant performance gain from enabling code-based visual reasoning.

Ablation Setting	Text		Multimodal		Overall	
	PS	AC	PS	AC	PS	AC
Qwen-2.5VL-3B	33.4	7.9	23.6	3.6	27.5	5.3
Qwen-2.5VL-3B-Text-Tune	34.3	12.7	27.4	5.8	30.1	8.4
CodePlot-CoT-3B	35.5	13.6	29.3	7.4	31.8	9.9

Table 4: Comparing our code-driven paradigm against direct image generation VCoT. Bagel-Thinking-with-image is fine-tuned to generate direct image outputs in reasoning steps, while CodePlot-CoT-Bagel uses our code-generation paradigm. This validates the efficacy of our paradigm.

Ablation Setting	Text		Multimodal		Overall	
	PS	AC	PS	AC	PS	AC
Bagel	32.9	8.5	24.0	7.0	27.6	7.6
Bagel-Thinking-with-image	40.3	10.1	28.4	8.3	33.2	9.0
CodePlot-CoT-Bagel	43.1	11.9	31.1	10.2	35.9	10.9

5.5 ABLATION STUDIES

To better understand the contribution of each design choice in our framework, we conduct two sets of ablation experiments.

Text-only vs. Code-driven Visual Reasoning. We first compare our code-driven paradigm against text-only reasoning using Qwen-2.5VL-3B as the base model. To establish a text-only fine-tuned baseline, we remove all images from the solutions in our dataset and fine-tune the model exclusively on textual reasoning, resulting in Qwen-2.5VL-3B-Text-Tune. This model shows only marginal improvement over the vanilla baseline because it remains fundamentally constrained by its inability to incorporate visual information. In contrast, our CodePlot-CoT-3B achieves substantial gains, clearly demonstrating the advantage of introducing executable code for visual reasoning.

Code-driven vs. Direct Image Generation. We further investigate whether code-based visual reasoning is more effective than direct image generation in reasoning. Since Qwen-2.5-VL does not support image generation, we perform this comparison on the unified model Bagel. The Bagel-Thinking-with-image is fine-tuned to directly produce interleaved text–image outputs on our dataset. Although this approach provides some improvements, it underperforms our CodePlot-CoT-Bagel, which leverages structured executable code. These results validate that code-driven reasoning offers a more precise and controllable representation of visual thoughts than direct pixel-level generation.

6 CONCLUSION

In this work, we introduce CodePlot-CoT, a code-driven chain-of-thought paradigm that enables VLMs to “think with images” in mathematical reasoning. By representing visual reasoning as executable snippets of plotting code, our approach circumvents the limitations of pixel-level image generation, achieving precise and controllable visual thought. To achieve this paradigm, we construct Math-VR, the first large-scale bilingual dataset benchmark for mathematical visual reasoning, and develop MatplotCode, a high-fidelity image-to-code converter. Extensive experiments demonstrate that our model consistently outperforms baseline models with improvements of up to 21%. We have used GPT-5 to help refine grammar in this paper.

7 ETHICS AND REPRODUCIBILITY STATEMENT

All data used in this study are collected from publicly available websites, ensuring that no private or sensitive information is involved in the dataset construction. The details on dataset, benchmark construction and evaluation are presented in Section 3.2 and Section 3.3. Training and implementation details are described in Section 4.3. Additional information, including evaluation templates, manual verification processes, and further dataset construction details, is provided in the Appendix. These resources are made available to facilitate transparent assessment and to support reproducibility of our results.

8 ACKNOWLEDGMENTS

We would like to extend our special thanks to the following members for their participation in the manual verification of the benchmark: Manyuan Zhang and Yan Feng from Meituan, Kunming Luo and Yexin Liu from The Hong Kong University of Science and Technology, Zihao Pan from Sun Yat-sen University, Dian Zheng, Rongyao Fang, Kaituo Feng, and Yilei Jiang from CUHK, Zhangquan Chen from Tsinghua University, Yimeng Jia from Peking University, Hongyu Li from Beihang University and Zhekai Chen and Chengqi Duan and Kaiyue Sun from The University of Hong Kong.

REFERENCES

- Anthropic. Introducing claude 4. <https://www.anthropic.com/news/clause-4>, 2025.
- Shuai Bai, Keqin Chen, Xuejing Liu, Jialin Wang, Wenbin Ge, Sibo Song, Kai Dang, Peng Wang, Shijie Wang, Jun Tang, et al. Qwen2. 5-vl technical report. *arXiv preprint arXiv:2502.13923*, 2025.
- Xinyan Chen, Renrui Zhang, Dongzhi Jiang, Aojun Zhou, Shilin Yan, Weifeng Lin, and Hongsheng Li. Mint-cot: Enabling interleaved visual tokens in mathematical chain-of-thought reasoning. *arXiv preprint arXiv:2506.05331*, 2025.
- Ethan Chern, Zhulin Hu, Steffi Chern, Siqi Kou, Jiadi Su, Yan Ma, Zhijie Deng, and Pengfei Liu. Thinking with generated images. *arXiv preprint arXiv:2505.22525*, 2025.
- Gheorghe Comanici, Eric Bieber, Mike Schaeckermann, Ice Pasupat, Noveen Sachdeva, Inderjit Dhillon, Marcel Blistein, Ori Ram, Dan Zhang, Evan Rosen, et al. Gemini 2.5: Pushing the frontier with advanced reasoning, multimodality, long context, and next generation agentic capabilities. *arXiv preprint arXiv:2507.06261*, 2025.
- Charles Corbière, Simon Roburin, Syrielle Montariol, Antoine Bosselut, and Alexandre Alahi. Retrieval-based interleaved visual chain-of-thought in real-world driving scenarios. *arXiv preprint arXiv:2501.04671*, 2025.
- Google Deepmind. Introducing gemini 2.0: our new ai model for the agentic era. <https://blog.google/technology/google-deepmind/google-gemini-ai-update-december-2024/>, 2024.
- Google Deepmind. Introducing openai o3 and o4-mini. <https://deepmind.google/models/gemini/pro/>, 2025.
- Chaorui Deng, Deyao Zhu, Kunchang Li, Chenhui Gou, Feng Li, Zeyu Wang, Shu Zhong, Weihao Yu, Xiaonan Nie, Ziang Song, et al. Emerging properties in unified multimodal pretraining. *arXiv preprint arXiv:2505.14683*, 2025.
- Chengqi Duan, Rongyao Fang, Yuqing Wang, Kun Wang, Linjiang Huang, Xingyu Zeng, Hongsheng Li, and Xihui Liu. Got-r1: Unleashing reasoning capability of mllm for visual generation with reinforcement learning. *arXiv preprint arXiv:2505.17022*, 2025.
- Rongyao Fang, Chengqi Duan, Kun Wang, Linjiang Huang, Hao Li, Shilin Yan, Hao Tian, Xingyu Zeng, Rui Zhao, Jifeng Dai, et al. Got: Unleashing reasoning capability of multimodal large language model for visual generation and editing. *arXiv preprint arXiv:2503.10639*, 2025.
- Jiahui Gao, Renjie Pi, Jipeng Zhang, Jiacheng Ye, Wanjun Zhong, Yufei Wang, Lanqing Hong, Jianhua Han, Hang Xu, Zhenguo Li, et al. G-llava: Solving geometric problem with multi-modal large language model. *arXiv preprint arXiv:2312.11370*, 2023a.
- Luyu Gao, Aman Madaan, Shuyan Zhou, Uri Alon, Pengfei Liu, Yiming Yang, Jamie Callan, and Graham Neubig. Pal: Program-aided language models. In *International Conference on Machine Learning*, pp. 10764–10799. PMLR, 2023b.

-
- Google. Introducing gemini 2.5 flash image, our state-of-the-art image model. <https://developers.googleblog.com/en/introducing-gemini-2-5-flash-image/>, 2025.
- Daya Guo, Dejian Yang, Huawei Zhang, Junxiao Song, Ruoyu Zhang, Runxin Xu, Qihao Zhu, Shirong Ma, Peiyi Wang, Xiao Bi, et al. Deepseek-r1: Incentivizing reasoning capability in llms via reinforcement learning. *arXiv preprint arXiv:2501.12948*, 2025.
- Wenyi Hong, Wenmeng Yu, Xiaotao Gu, Guo Wang, Guobing Gan, Haomiao Tang, Jiale Cheng, Ji Qi, Junhui Ji, Lihang Pan, et al. Glm-4.1 v-thinking: Towards versatile multimodal reasoning with scalable reinforcement learning. *arXiv e-prints*, pp. arXiv–2507, 2025.
- Yushi Hu, Weijia Shi, Xingyu Fu, Dan Roth, Mari Ostendorf, Luke Zettlemoyer, Noah A Smith, and Ranjay Krishna. Visual sketchpad: Sketching as a visual chain of thought for multimodal language models. *Advances in Neural Information Processing Systems*, 37:139348–139379, 2024.
- Chaoya Jiang, Yongrui Heng, Wei Ye, Han Yang, Haiyang Xu, Ming Yan, Ji Zhang, Fei Huang, and Shikun Zhang. Vlm-r³: Region recognition, reasoning, and refinement for enhanced multimodal chain-of-thought. *arXiv preprint arXiv:2505.16192*, 2025.
- Ang Li, Charles Wang, Kaiyu Yue, Zikui Cai, Ollie Liu, Deqing Fu, Peng Guo, Wang Bill Zhu, Vatsal Sharan, Robin Jia, et al. Zebra-cot: A dataset for interleaved vision language reasoning. *arXiv preprint arXiv:2507.16746*, 2025a.
- Chengzu Li, Wenshan Wu, Huanyu Zhang, Yan Xia, Shaoguang Mao, Li Dong, Ivan Vulić, and Furu Wei. Imagine while reasoning in space: Multimodal visualization-of-thought. *arXiv preprint arXiv:2501.07542*, 2025b.
- Pan Lu, Hritik Bansal, Tony Xia, Jiacheng Liu, Chunyuan Li, Hannaneh Hajishirzi, Hao Cheng, Kai-Wei Chang, Michel Galley, and Jianfeng Gao. Mathvista: Evaluating mathematical reasoning of foundation models in visual contexts. *arXiv preprint arXiv:2310.02255*, 2023.
- MathArena. hmmt-feb-2025. https://huggingface.co/datasets/MathArena/hmmt_feb_2025, 2025.
- OpenAI. Gpt-4o system card. <https://openai.com/index/gpt-4o-system-card/>, 2024.
- OpenAI. Introducing gpt-4.1 in the api. <https://openai.com/index/gpt-4-1/>, 2025a.
- OpenAI. Introducing openai o3 and o4-mini. <https://openai.com/index/introducing-o3-and-o4-mini/>, 2025b.
- Kaihang Pan, Yang Wu, Wendong Bu, Kai Shen, Juncheng Li, Yingting Wang, Yunfei Li, Siliang Tang, Jun Xiao, Fei Wu, et al. Unlocking aha moments via reinforcement learning: Advancing collaborative visual comprehension and generation. *arXiv preprint arXiv:2506.01480*, 2025.
- Bytedance Seed. Seed1.6 tech introduction. https://seed/bytedance.com/en/seed1_6, 2025.
- Hao Shao, Shengju Qian, Han Xiao, Guanglu Song, Zhuofan Zong, Letian Wang, Yu Liu, and Hongsheng Li. Visual cot: Advancing multi-modal language models with a comprehensive dataset and benchmark for chain-of-thought reasoning. *Advances in Neural Information Processing Systems*, 37:8612–8642, 2024.
- Wenhao Shi, Zhiqiang Hu, Yi Bin, Junhua Liu, Yang Yang, See-Kiong Ng, Lidong Bing, and Roy Ka-Wei Lee. Math-lava: Bootstrapping mathematical reasoning for multimodal large language models. *arXiv preprint arXiv:2406.17294*, 2024.
- Dídac Surís, Sachit Menon, and Carl Vondrick. Vipergrpt: Visual inference via python execution for reasoning. In *Proceedings of the IEEE/CVF international conference on computer vision*, pp. 11888–11898, 2023.

-
- Gemma Team, Aishwarya Kamath, Johan Ferret, Shreya Pathak, Nino Vieillard, Ramona Merhej, Sarah Perrin, Tatiana Matejovicova, Alexandre Ramé, Morgane Rivière, et al. Gemma 3 technical report. *arXiv preprint arXiv:2503.19786*, 2025.
- vals.ai. Aime benchmark. <https://www.vals.ai/benchmarks/aime-2025-09-08>, 2025a.
- vals.ai. Math 500 benchmark. <https://www.vals.ai/benchmarks/math500-08-26-2025>, 2025b.
- Ke Wang, Houxing Ren, Aojun Zhou, Zimu Lu, Sichun Luo, Weikang Shi, Renrui Zhang, Linqi Song, Mingjie Zhan, and Hongsheng Li. Mathcoder: Seamless code integration in llms for enhanced mathematical reasoning. *arXiv preprint arXiv:2310.03731*, 2023.
- Ke Wang, Junting Pan, Weikang Shi, Zimu Lu, Houxing Ren, Aojun Zhou, Mingjie Zhan, and Hongsheng Li. Measuring multimodal mathematical reasoning with math-vision dataset. *Advances in Neural Information Processing Systems*, 37:95095–95169, 2024.
- Ke Wang, Junting Pan, Linda Wei, Aojun Zhou, Weikang Shi, Zimu Lu, Han Xiao, Yunqiao Yang, Houxing Ren, Mingjie Zhan, et al. Mathcoder-vl: Bridging vision and code for enhanced multimodal mathematical reasoning. *arXiv preprint arXiv:2505.10557*, 2025a.
- Peijie Wang, Zhong-Zhi Li, Fei Yin, Dekang Ran, and Cheng-Lin Liu. Mv-math: Evaluating multimodal math reasoning in multi-visual contexts. In *Proceedings of the Computer Vision and Pattern Recognition Conference*, pp. 19541–19551, 2025b.
- Weiyun Wang, Zhangwei Gao, Lixin Gu, Hengjun Pu, Long Cui, Xingguang Wei, Zhaoyang Liu, Linglin Jing, Shenglong Ye, Jie Shao, et al. Internvl3. 5: Advancing open-source multimodal models in versatility, reasoning, and efficiency. *arXiv preprint arXiv:2508.18265*, 2025c.
- Yikun Wang, Siyin Wang, Qinyuan Cheng, Zhaoye Fei, Liang Ding, Qipeng Guo, Dacheng Tao, and Xipeng Qiu. Visuothink: Empowering l1vm reasoning with multimodal tree search. *arXiv preprint arXiv:2504.09130*, 2025d.
- Jason Wei, Xuezhi Wang, Dale Schuurmans, Maarten Bosma, Fei Xia, Ed Chi, Quoc V Le, Denny Zhou, et al. Chain-of-thought prompting elicits reasoning in large language models. *Advances in neural information processing systems*, 35:24824–24837, 2022.
- Biao Yang, Bin Wen, Boyang Ding, Changyi Liu, Chenglong Chu, Chengru Song, Chongling Rao, Chuan Yi, Da Li, Dunju Zang, et al. Kwai keye-vl 1.5 technical report. *arXiv preprint arXiv:2509.01563*, 2025.
- Guanghao Zhang, Tao Zhong, Yan Xia, Zhelun Yu, Haoyuan Li, Wanggui He, Fangxun Shu, Mushui Liu, Dong She, Yi Wang, et al. Cmmcot: Enhancing complex multi-image comprehension via multi-modal chain-of-thought and memory augmentation. *arXiv preprint arXiv:2503.05255*, 2025.
- Renrui Zhang, Dongzhi Jiang, Yichi Zhang, Haokun Lin, Ziyu Guo, Pengshuo Qiu, Aojun Zhou, Pan Lu, Kai-Wei Chang, Yu Qiao, et al. Mathverse: Does your multi-modal l1lm truly see the diagrams in visual math problems? In *European Conference on Computer Vision*, pp. 169–186. Springer, 2024a.
- Renrui Zhang, Xinyu Wei, Dongzhi Jiang, Ziyu Guo, Shicheng Li, Yichi Zhang, Chengzhuo Tong, Jiaming Liu, Aojun Zhou, Bin Wei, et al. Mavis: Mathematical visual instruction tuning with an automatic data engine. *arXiv preprint arXiv:2407.08739*, 2024b.
- Aojun Zhou, Ke Wang, Zimu Lu, Weikang Shi, Sichun Luo, Zipeng Qin, Shaoqing Lu, Anya Jia, Linqi Song, Mingjie Zhan, et al. Solving challenging math word problems using gpt-4 code interpreter with code-based self-verification. *arXiv preprint arXiv:2308.07921*, 2023.

A DATASET

A.1 DATA COLLECTION

We first collect approximately 900k secondary school-level mathematical problems and their corresponding solutions from public websites. Each sample contains at least one image in the solution explanation. These images vary in nature: some consist solely of texts about the problem, others depict mathematical figures such as geometric diagrams or function plots, while a portion are non-informative or irrelevant images. We label these images with Qwen2.5-VL-72B and retain only those questions containing mathematical images and discard the rest. To improve readability and ensure dataset consistency, we leverage GPT-4.1 to extract text from the remaining purely textual images. Subsequently, we task GPT-4.1 to rewrite each original sample into two standardized markdown files, representing the question and solution separately. In the final step, GPT-4.1 verifies these files to identify and remove incomplete or incoherent samples. Furthermore, to improve the accessibility of our dataset, we use GPT-4.1 to translate the samples into English, resulting

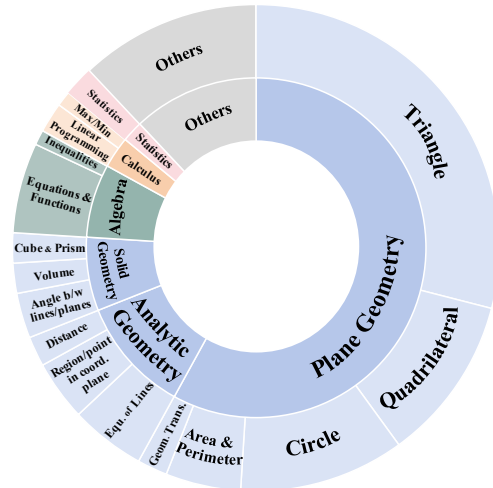


Figure 6: **Distribution of Knowledge Types in Math-VR Dataset.** Geometry constitutes the majority of problems (76%), with Algebra and Calculus comprising 12%.

in 178,150 bilingual question-solution pairs.

A.2 DATASET CATEGORIZATION

In Math-VR dataset, approximately 29% of the questions are expressed using text only, while the remaining 71% are demonstrated with both text and mathematical images. Both types of questions require visual mathematical reasoning. In addition to organizing our dataset based on the modality of the questions, we can also classify them according to different knowledge types. First, we randomly sample several thousand question-solution pairs and input them into an VLM (here, GPT-4.1), which generates initial labels including a root knowledge type, a sub-knowledge type and a primary knowledge point, for each pair. Using these labels alongside formal definitions of mathematical concepts, we construct a hierarchical knowledge tree. This taxonomy then serves as a framework to categorize all 90k unique samples in our dataset. Based on this categorization, the dataset is divided into four main knowledge domains: Geometry, Algebra, Calculus, and Statistics. Geometry constitutes the largest portion, 81% of all samples. Within Geometry, there are three primary subcategories: Plane Geometry, Solid Geometry, and Analytic Geometry. These subcategories are further broken down into specific knowledge points such as Triangle, Circle, Quadrilateral, and Area & perimeter calculation. This hierarchical categorization is visually summarized in the pie chart shown in Figure 6.

Table 5: Key Statistics for Math-VR Dataset

Statistics	Number
Total Unique Samples	89,075
- Training	86,575
- Testing	2500
- Text questions	29%
- Multimodal questions	71%
- Single-part questions	51%
- Multiple-choice	40%
- Answer-based	55%
- Proof-based	5%
- Multi-part questions	49%
- Multiple-choice	3%
- Answer-based	72%
- Proof-based	25%
- Two sub-questions	51%
- Three sub-questions	40%
- Four sub-questions	7%
Question length (text tokens)	
- Average	131.64
Solution length (text tokens)	
- Average	510.76
Multimodal Question Image	
- Average number	1.05
- Average resolution	208x139
Solution Image	
- Average number	1.15
- Average resolution	199x151

A.3 DATASET STATISTICS

We summarize the statistics of our dataset in Table 5. The dataset comprises approximately 90k unique questions covering a wide range of types, including both single-part and multipart questions, with two- and three-part questions being the most common. It also includes multiple-choice, answer-based, and proof-based questions, among which answer-based questions are the most prevalent. On average, each solution contains at least one image, reflecting the importance of using images to support the reasoning process.

B BENCHMARK

B.1 TEMPLATES USED IN VLM-BASED EVALUATION PIPELINE

We use GPT-4.1 as our VLM evaluation tool. Figure 7 presents the template we use to prompt the VLM for generating the meta information of each sample. Figure 8 displays the template used by the VLM to evaluate the model response to each question.

B.2 MANUAL SAMPLE SELECTION AND META INFORMATION VERIFICATION

We combine the selection of samples that require non-trivial visual reasoning with the verification of meta information into a single manual review process. Figure 9 shows the interface used for this review. The interface displays the question, solution, and meta information all within one view. Annotators are tasked with flagging the unqualified samples. For the remaining samples, they verify that the extracted answers match the final answers in the ground-truth solutions, and that the identified scoring points and their values are reasonable and consistent. All manual verifications involved in constructing the benchmark are performed by 15 senior college students majoring in STEM disciplines.

C TRAINING DETAILS

We leverage Qwen2.5VL-32B-Instruct as the base model for both MatPlotCode and the CodePlot-CoT model. During training, we pad all input images into squares before resizing them randomly with lengths between 224 and 560. For rendered images in reasoning chain, we pad and embed them at a fixed resolution of 448×448. The training for MatPlotCode is a two-stage process: we first align the visual components by training only the vision encoder (ViT) and the MLP projector for one epoch, and then perform full-parameter fine-tuning for an additional two epochs. We use a batch size of 512 and a learning rate of 2e-5. For the main CodePlot-CoT model, we initialize its weights from our vision-aligned converter after the completion of Stage 1. We then fine-tune this model on our curated SFT dataset for 5000 steps, using a batch size of 256 and a learning rate of 3e-5. All settings are conducted on 32 NVIDIA H200 GPUs, with each training stage taking approximately 36 hours.

D CODEPLOT-COT SAMPLES ON MATH-VR BENCHMARK

We present some samples of CodePlot-CoT on Math-VR Benchmark in Figure 12 and 13. Figure 12 includes a math figure in input, while Figure 13 is purely text-based inputs. However, both problems require visual reasoning. As shown, our model demonstrates strong reasoning capabilities in both textual and visual reasoning, highlighting our code-driven visual reasoning paradigm.

E LIMITATIONS

Due to the limitations of data scale and model size, our MatPlotCode has not yet achieved a 100% fidelity rate on images-to-code conversion, which means that some visual reasoning images are not entirely accurate. As a result, our final model may also produce slightly imperfect visual reasoning in certain problems. For instance, in Figure 14, point H should lie on edge AD, but the generated image shows a slight displacement. We hope that future work will further advance the task of image-to-code conversion, thereby enabling a more robust realization of our paradigm.

<USER> : I will give you the question, analysis, and answer of a mathematical problem with the ID: {**id**}. The problem may consist of a single question or multiple sub-questions.

1. Summarize the Answers: Clearly summarize all answers for the entire problem. Indicate how many answers there are and specify which answer corresponds to which question or sub-question.
2. List Scoring Points: For each question or sub-question, identify the scoring points. Scoring points are the critical steps needed to solve the problem, such as applying theorems, making necessary reasoning steps, or performing correct calculations. Please assign a score (e.g., 1, 2) for each scoring point based on its difficulty

Present your answer in the following JSON format: { "id": [question id], "scoring_points": [here should be a dictionary with scoring points: 'p1': [scoring point 1], 'p2': [scoring point 2], ...], "scores": [here should be a dictionary with scores for the scoring points: 's1': [score for p1], 's2': [score for p2], ...], "total_answer": [the number of all answers], "answer_summary": [here should be a dictionary, the keys should match the questions, the values should be the answers]}

...Question...

```
<ASSISTANT> :
{
  "id": 25006,
  "scoring_points": {
    "p1": "Recognize that AB is the diameter, thus angles ACB and ADB are right angles by the inscribed angle theorem.",
    "p2": "Apply the Pythagorean theorem to calculate BC in triangle ACB and BD in triangle ADB.",
    "p3": "Determine that triangle ABC is an isosceles right triangle to find angle BAC.",
    "p4": "Determine angle BAD in triangle ABD using calculated lengths.",
    "p5": "Classify the different configurations (AC and AD on the same or opposite sides of AB), and compute corresponding values for angle CAD.",
    "p6": "Combine stepwise results to conclude that the possible values for angle CAD are 15° or 75°."
  },
  "scores": { "s1": 1, "s2": 2, "s3": 1, "s4": 1, "s5": 2, "s6": 1 },
  "total_answer": 1,
  "answer_summary": { "1": "The possible values of angle CAD are 15° or 75°." },
  "max_score": 8
}
```

Figure 7: **Template used by GPT-4.1 to generate meta information for evaluation.** The text highlighted in cyan should be replaced with information of the specific question.

<USER> : You are an expert math teacher and grader. Your task is to evaluate a student's solution to a mathematical question and provide a score. You will be provided with the mathematical question (which may include multiple sub-questions), its ID, the student's solution, the correct answer, and the maximum possible score for the question below:

...Question...

```
{ 'id':{question_id}, 'student_solution':{model_response},
  'correct_answer':{correct_answer}, 'max_score':{max_score} }.
```

Please follow these steps precisely:

1. Initial Check for Correctness:

- Thoroughly review the question and the student_solution to identify the student's final answer.
- Compare this final answer directly with the provided correct_answer.
- If the answers match exactly, award the full max_score.

2. Partial Credit Evaluation:

- If the student's answer is not fully correct, evaluate its work for partial credit using the grading rubric: {'scoring_points':{scoring_points}, 'point_values':{point_values}}.
- Go through each scoring_point, indicate if the student successfully completed that step.
- Write down all the point_ids that the student earned and calculate the total score by summing the values of those points.

3. Provide your evaluation in a strict JSON format:

```
{ "id": "string",
  "question_solution_analysis": "string"
  "is_fully_correct": "boolean",
  "check_scoring_point": "string",
  "awarded_points": ["all" OR a list of earned point_ids like "p1", "p2"],
  "final_score": "number" }
```

Field Explanations:

- "id": question id.
- "question_solution_analysis": Analyze the question requirements and compare the student's answer against the correct_answer."
- "is_fully_correct": True if the student's solution is fully correct, otherwise False.
- "check_scoring_point": If fully correct, provide an empty string """. If not fully correct, explain where in the student_solution each scoring point is fully met or not met.
- "awarded_points": If fully correct, this should be ["all"]. If partially correct, provide a list containing the fully met point_ids (e.g., ["p1", "p3"]). If no points met, provide an empty list [].
- "final_score": the max_score if fully correct, or the sum of partial scores otherwise.

Figure 8: **Template used by GPT-4.1 to evaluate model response.** The text highlighted in cyan should be replaced with information of the specific question. The orange model_response should be replaced with the response generated by the question.

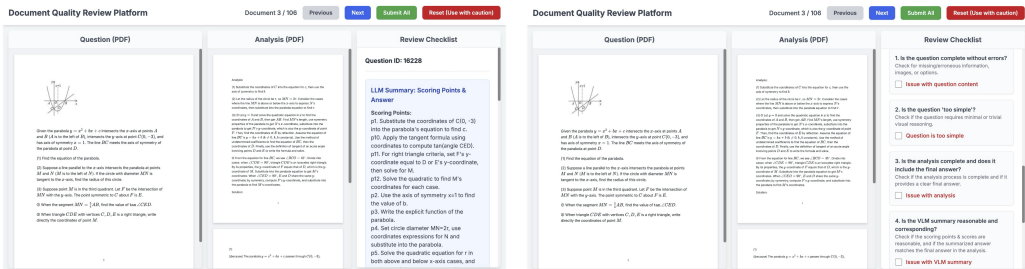
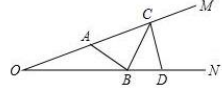


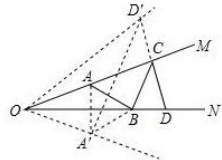
Figure 9: **The GUI interface for manual sample selection and meta information verification.** This interface displays the Question and Analysis files on the left and center panels, with the Review Checklist on the right. **Left:** The meta information extracted for each sample is displayed on the right panel. **Right:** Scrolling down reveals the items for annotators to check and flag.

Math-VR Example:**Question:**

As shown, $\angle MON = 20^\circ$, A is a point on ray OM with $OA = 4$, D is a point on ray ON with $OD = 8$, C is any point on ray AM , and B is any point on segment OD . Find the minimum value of the length $AB + BC + CD$ of the broken line $ABCD$.

**Analysis:**

Construct the symmetric points A' and D' of A and D with respect to ON and OM , respectively, and connect $A'B$, CD' , $A'D'$, OD' , and OA' .



Then $A'B = AB$, $CD' = CD$, so

$$AB + BC + CD \geq A'B + BC + CD'.$$

Clearly,

$$A'B + BC + CD' \geq A'D'.$$

Since $\angle A'ON = \angle NOM = \angle MOD' = 20^\circ$, we have $\angle D'OA' = 60^\circ$.

Also, $OA' = OA = 4$, $OD' = OD = 8$, thus

$$\frac{OA'}{OD'} = \frac{1}{2}.$$

And since $\cos 60^\circ = \frac{1}{2}$, we have

$$\cos 60^\circ = \frac{OA'}{OD'},$$

which shows that $\triangle D'OA'$ is a right triangle, with $\angle OA'D' = 90^\circ$.

Hence,

$$A'D' = \sqrt{OD'^2 - OA'^2} = \sqrt{8^2 - 4^2} = \sqrt{64 - 16} = \sqrt{48} = 4\sqrt{3}.$$

Answer: $4\sqrt{3}$.

Figure 10: Multimodal input sample from Math-VR.

Math-VR Example:

Question:

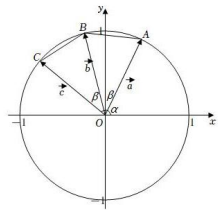
Let the plane vectors $\vec{a} = (\cos \alpha, \sin \alpha)$, $\vec{b} = (\cos(\alpha + \beta), \sin(\alpha + \beta))$, $\vec{c} = (\cos(\alpha + 2\beta), \sin(\alpha + 2\beta))$, where $0^\circ < \beta < 180^\circ$. Then ()

Options:

- A. $|\vec{a} - \vec{b}| = |\vec{b} - \vec{c}|$
- B. $(\vec{a} + \vec{c}) \parallel \vec{b}$
- C. If $|\vec{a} + \vec{c}| = |\vec{b}|$, then $\beta = 30^\circ$
- D. If $\vec{a} + \vec{b} + \vec{c} = \vec{0}$, then $\beta = 120^\circ$

Analysis:

Because $|\vec{a}| = |\vec{b}| = |\vec{c}| = 1$, we plot $\overrightarrow{OA} = \vec{a}$, $\overrightarrow{OB} = \vec{b}$, $\overrightarrow{OC} = \vec{c}$ respectively on the unit circle.

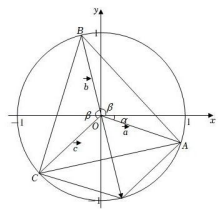


(A) $|\vec{a} - \vec{b}| = |AB|$, $|\vec{b} - \vec{c}| = |BC|$. Since $\angle AOB = \angle BOC = \beta$, we have $|AB| = |BC|$, i.e. $|\vec{a} - \vec{b}| = |\vec{b} - \vec{c}|$. Therefore, **A is correct**.

(B) Because $\angle AOB = \angle BOC = \beta$, OB is the angle bisector of OA and OC , and $OA = OC = 1$. By the vector addition rule, $(\vec{a} + \vec{c}) \parallel \vec{b}$. Therefore, **B is correct**.

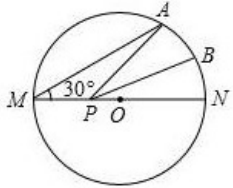
(C) When $\beta = 60^\circ$, $\triangle OAB$ and $\triangle BOC$ are both equilateral triangles. By the parallelogram rule, $\vec{a} + \vec{c} = \vec{b}$, hence $|\vec{a} + \vec{c}| = |\vec{b}|$. Thus, $\beta = 60^\circ$, not 30° , so **C is incorrect**.

(D) Let $(\vec{a} + \vec{c}) = \lambda \vec{b}$, $\lambda \in R$. If $\vec{a} + \vec{b} + \vec{c} = \vec{0}$, then $(\lambda + 1) \vec{b} = 0$, giving $\lambda = -1$. At this point, by the vector rule, $\triangle ABC$ is equilateral, so $\beta = 120^\circ$. Hence, **D is correct**.



Therefore, the correct options are: **A, B, D**.

Figure 11: Text input example from Math-VR.

Model Generated Example:**Question:**

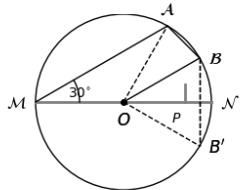
As shown, MN is the diameter of circle $\odot O$ and the radius of $\odot O$ is 2. Point A lies on $\odot O$ and $\angle AMN = 30^\circ$. B is the midpoint of arc AN . P is a movable point on the diameter MN . Find the minimum value of $PA + PB$: _____.

Analysis:

Reflect point B across line MN to get point B' , and connect AB' . By the property of axial symmetry, AB' gives the minimum value of $PA + PB$. From the properties of central and inscribed angles subtending the same arc:

- $\angle AON = 2\angle AMN = 2 \times 30^\circ = 60^\circ$,
- By symmetry, $\angle B'ON = \angle BON = 30^\circ$.

With these, calculate the measure of $\angle AOB'$, then use the Pythagorean theorem to obtain the answer.

Solution:

Reflect point B across MN to get B' , and connect OA , OB , OB' , and AB' . The intersection of AB' with MN is the location where $PA + PB$ attains its minimum, thus $PA + PB$ minimum = AB' .

$$\angle AON = 2\angle AMN = 2 \times 30^\circ = 60^\circ$$

B is the midpoint of arc AN :

$$\angle BON = \frac{1}{2} \times 60^\circ = 30^\circ$$

By symmetry:

$$\angle B'ON = \angle BON = 30^\circ$$

$$\angle AOB' = \angle AON + \angle B'ON = 60^\circ + 30^\circ = 90^\circ$$

Thus $\triangle AOB'$ is an isosceles right triangle:

$$AB' = \sqrt{2} \cdot OA = 2\sqrt{2}$$

Answer: $2\sqrt{2}$

Figure 12: A multimodal math question form Math-VR benchmark and CodePlot-CoT generated analysis.

Model Generated Example:**Question:**

For an isosceles triangle $\triangle ABC$ with a perimeter of 36 cm, if the altitude to its base BC is 12 cm, what is the value of $\cos B$?

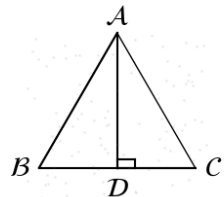
- A. $\frac{1}{2}$ B. $\frac{3}{2}$ C. $\frac{12}{13}$ D. $\frac{5}{13}$

Problem Analysis:

Let $AB = x$ cm, then $AC = AB = x$ cm, and $BC = (36 - 2x)$ cm. Calculate $BD = DC = \frac{1}{2}BC = (18 - x)$ cm. In right triangle ABD , by the Pythagorean theorem, we have:

$$x^2 = 12^2 + (18 - x)^2.$$

Solving gives $x = 13$, that is, $AB = 13$ cm, $BD = 5$ cm.

Problem Explanation

Let $AB = x$ cm, then $AC = AB = x$ cm, and $BC = (36 - 2x)$ cm. Since $AB = AC$ and AD is the altitude, so $BD = DC = \frac{1}{2}BC = (18 - x)$ cm. In right triangle ABD , by the Pythagorean theorem:

$$AB^2 = AD^2 + BD^2.$$

That is,

$$x^2 = 12^2 + (18 - x)^2.$$

Solving gives $x = 13$. So $AB = 13$ cm, $BD = 5$ cm. Thus $\cos B = \frac{BD}{AB} = \frac{5}{13}$. Therefore, the answer is D.

Figure 13: A pure textual math question form Math-VR benchmark and CodePlot-CoT generated analysis.

Model Generated Example:

Question:

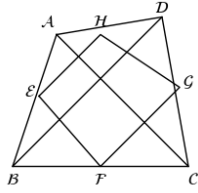
If the diagonals of a quadrilateral are equal, then the quadrilateral formed by sequentially connecting the midpoints of its sides must be _____.

- Options: A. Trapezoid B. Rectangle C. Rhombus D. Square

Analysis:

Given that the diagonals of the quadrilateral are equal, by the Midline Theorem of triangles, it follows that all four sides of the resulting quadrilateral are equal, so the quadrilateral formed is a rhombus.

Solution:



As shown in the figure, $AC = BD$, and E, F, G, H are the midpoints of segments AB , BC , CD , and AD , respectively.

Since EH and FG are the midlines of $\triangle ABD$ and $\triangle BCD$, respectively, and EF and HG are the midlines of $\triangle ACD$ and $\triangle ABC$, respectively,

$$EH = FG = \frac{1}{2}BD, \quad EF = HG = \frac{1}{2}AC$$

Since $AC = BD$

$$EH = FG = EF = HG$$

Therefore, quadrilateral $EFGH$ is a rhombus. Thus, the answer is C.

Answer: C. Rhombus

Figure 14: A pure textual math question form Math-VR benchmark and CodePlot-CoT generated solution. The textual reasoning is correct, but the model generates a slightly imperfect image in reasoning by placing H not on edge AD.